Tracking Single Proteins within Cells

Mark Goulian and Sanford M. Simon

Laboratory of Cellular Biophysics, The Rockefeller University, New York, New York 10021 USA

ABSTRACT   We present experiments in which single proteins were imaged and tracked within mammalian cells. Single proteins of R-phycoerythrin (RPE) were imaged by epifluorescence microscopy in the nucleoplasm and cytoplasm at 71 frames/s. We acquired two-dimensional trajectories of proteins (corresponding to the projection of three-dimensional trajectories onto the plane of focus) for an average of 17 frames in the cytoplasm and 16 frames in the nucleus. Diffusion constants were determined from linear fits to the mean square displacement and from the mean displacement squared per frame. We find that the distribution of diffusion constants for RPE within cells is broader than the distributions obtained from RPE in a glycerol solution, from a Monte Carlo simulation, and from the theoretical distribution for simple diffusion. This suggests that on the time scales of our measurements, the motion of single RPE proteins in the cytoplasm and nucleoplasm cannot be modeled by simple diffusion with a unique diffusion constant. Our results demonstrate that it is possible to follow the motion of single proteins within cells and that the technique of single molecule tracking can be used to probe the dynamics of intracellular macromolecules.

INTRODUCTION

As we move toward a more integrative view of cellular function, there is an increasing need to develop an accurate picture of the underlying microenvironment within the cell. It is clear that protein localization is crucial for accurate processing of cell signals, but little is known about how molecules manage to end up at the right place at the right time. Are macromolecules able to diffuse sufficiently rapidly to explore the full volume of the cell and find their destination? For large complexes, at what size must motors or other means of directed transport be employed for efficient targeting? Do mobilities vary with position in the cell and are they modulated? Questions such as these must be addressed before cellular processes can be accurately modeled. Using fluorescence recovery after photobleaching (FRAP) (Wolf, 1989) and related techniques, it has been found that macromolecules have significantly lower intracellular diffusion constants (D_c) compared with the corresponding diffusion constants in free (aqueous) solution (D_w). This is in contrast to the case of small molecules, which appear to have comparable mobilities inside the cell and in water (Fushimi and Verkman, 1991; Luby-Phelps et al., 1993). A number of groups have found that D_c/D_w decreases with increasing molecular weight for a variety of macromolecules and cell types (Luby-Phelps et al., 1986, 1987; Lang et al., 1986; Arrio-Dupont et al., 1996, 2000; Lukacs et al., 2000), leading to models in which the cytoskeleton and other cellular components act as sieves (reviewed in Luby-Phelps, 1994, 2000). Other experiments, however, indicate that D_c/D_w is independent of molecular

weight, with $D_c \approx D_w/4$, at least for measurements over short time scales (Seksek et al., 1997; Politz et al., 1998).

Most FRAP experiments have been analyzed in terms of a single diffusion constant. However, more complex diffusive behavior will not always be apparent in photobleaching data (Gordon et al., 1995; Periasamy and Verkman, 1998). An alternative technique, which is more sensitive to variations in particle dynamics, is single particle tracking. With this technique, the increase in sensitivity is gained at the expense of statistical sample size; the number of particles analyzed in tracking experiments is far smaller than the number of particles that contribute to the average quantities measured in a typical photobleaching experiment. Single particle tracking has been applied to two-dimensional diffusion in the plasma membrane and has provided evidence for a wide range of dynamics, including normal, confined, and anomalous diffusion, as well as directed motion (reviewed in Saxton and Jacobson, 1997). Recently, single particle tracking of particles diffusing in three dimensions in colloidal systems has been used to probe dynamics near the glass transition (Kegel and van Blaaderen, 2000; Weeks et al., 2000).

In this paper we describe the tracking of single proteins in the cytoplasm and nucleoplasm of mammalian cells. We use R-phycoerythrin (RPE), which is a 240-kDa autofluorescent protein consisting of seven subunits and ~30 chromophores (reviewed in Glazer, 1982, 1988). As shown by x-ray diffraction and electron microscopy, the protein has the shape of a disk with a diameter of 11 nm and a thickness of 6 nm (Ficner et al., 1992, and references therein). Because of the high quantum yield and extinction coefficient of RPE, single proteins can be imaged with a standard epifluorescence microscope. RPE has previously been used to track the motion of labeled membrane proteins (Wilson et al., 1996) and to identify membrane-protein clustering (Cherry et al., 1998). After microinjecting RPE into cells, we were able to track the proteins in two dimensions (the projection of the

three-dimensional trajectory onto the plane of focus) for an average of 17 frames in the cytoplasm and 16 frames in the nucleus, at 14 ms/frame. We determined diffusion constants from an analysis of mean squared displacements for each trajectory. By comparing our results to the distributions obtained for diffusion of RPE in a glycerol solution and from a Monte Carlo simulation, as well as to theoretical distributions, we find that the distribution of intracellular diffusion constants is too broad to be accounted for by statistical fluctuations. We conclude that over the time scales of our measurements, the motion of RPE is not described by simple diffusion with a unique diffusion constant in either the cytoplasm or the nucleoplasm. These experiments describe the first time that trajectories of single proteins have been followed within cells and demonstrate that single molecule tracking is an effective tool for exploring intracellular dynamics.

MATERIALS AND METHODS

Cell culture

TC7 cells, an African green monkey kidney epithelial cell line, were a gift from D. Dean (University of South Alabama). Cells were cultured on homemade coverslip chambers in Dulbecco's Modified Eagle's medium at 37°C with 5% CO_2. The coverslip chambers consisted of 60-mm polystyrene Petri dishes with ~1.5-cm holes drilled in the bottom and 22 mm × 22 mm no. 1.5 coverslips (Fisher Scientific, Pittsburgh, PA) glued over the holes with 734 RTV sealant (Dow Corning, Midland, MI). Grids were scratched into the coverslips to aid in locating injected cells. Before we viewed cells on the microscope, the medium, which was quite autofluorescent, was replaced with Hanks' balanced salt solution containing 20 mM HEPES (pH 7.4) (Freshney, 1994).

Phycoerythrin

R-Phycoerythrin (RPE) (Molecular Probes, Eugene, OR), which was obtained as an ammonium sulfate precipitate, was dialyzed against 100 mM sodium phosphate, 150 mM sodium chloride (pH 7.2) at 4°C with multiple changes of the dialysis solution. The RPE solution was then spun through a 0.2-μm sterile filter and stored at 4°C. The diffusion constant and monodispersity of RPE were determined with a DynaPro-801 dynamic light scattering instrument (Protein Solutions, Charlottesville, VA). The peptide CYTPPKKKRKVED, which contains the nuclear localization sequence (NLS) from the SV-40 large-T antigen, was synthesized at the Rockefeller University peptide synthesis facility. NLS was conjugated to RPE with the cross-linker Sulfo-SMCC (Pierce, Rockford, IL), following the manufacturer's protocols. The RPE-NLS product was dialyzed into 100 mM sodium phosphate, 150 mM sodium chloride (pH 7.2). From the shift of RPE-NLS relative to RPE on sodium dodecyl sulfate polyacrylamide gels, we estimate that each protein contained 10–20 NLS peptides (data not shown).

Microinjection

Micropipettes were pulled from borosilicate glass (1 mm outer diameter, 0.78 mm inner diameter) (Sutter, Novato, CA) on a P-87 puller (Sutter). Pulled pipettes were back-filled with a few microliters of the injection solution and then topped off with light mineral oil (Sigma, St. Louis, MO) to prevent capillary suction of buffer into the pipette. The protein concentration in the injection solution was ~30 μg/ml. Injection pressure was controlled by a Picospritzer II (General Valve, Fairfield, NJ) and was in the range of 10–25 kPa. RPE was injected into the cytoplasm or nucleus as indicated. RPE-NLS was injected into the cytoplasm, and the cells were incubated for 1 h at 37°C with 5% CO_2 to allow for efficient nuclear import.

RPE in glycerol solution

RPE was diluted to ~0.3 μg/ml in a solution consisting of 1 mg/ml bovine serum albumin (Sigma), 100 mM sodium phosphate, 150 mM sodium chloride (pH 7.2). Glyercol was then added to a concentration of 50% (by weight), and a small amount of 0.2 μm red fluorescent microspheres (Molecular Probes) was added to aid in focusing. Three microliters of this solution was deposited on a microscope slide, and a 18 mm × 18 mm no. 1.5 coverslip (Fisher Scientific) was placed on top. The edges of the coverslip were sealed with paraffin.

Microscopy

Microscopy was carried out at room temperature (~23°C) on an Olympus IX-70 inverted microscope (Olympus, Melville, NY) with a 100× UplanApo lens (NA 1.35) (Olympus), equipped with a HQ545/30 excitation, Q565LP dichroic, HQ610/75 emission filter cube (Omega, Brattleboro VT). Illumination for fluorescence was provided by a 150-W xenon lamp (Optiquip, Highland Mills, NY). Images were acquired with an I-Pentamax-512EFT intensified charged-coupled device camera (512 × 512, 15 μm × 15 μm pixels) (Princeton Instruments, Trenton, NJ) cooled to −25°C, with the intensifier gain at 50%. A region of interest of size ~73 pixels × 100 pixels was defined, and sequences consisting of 250 consecutive Δt = 14.09 ms exposures (71 frames/s) were acquired into memory of a PC, using the image acquisition program WinView 32 (Princeton Instruments).

Image analysis

Particle tracking and analysis were carried out with our own software written in C and LabView (National Instruments, Austin TX), using the IMAQ Vision (National Instruments) and AVI (ImageMill Technology, Mirmande, France) libraries on a PC. Images were smoothed by averaging each pixel with its eight nearest neighbors, and the location of each particle was taken to be at the center of mass of the intensity maxima. For each particle in a frame, a region of radius 10 pixels centered on the location of the particle, but no closer than one pixel from the frame boundary, was searched in the subsequent frame. If one and only one particle was found, and if the (distance)^2 from the center of the region was less than 40 pixels^2, then this particle was considered to have the same identity as the particle in the previous frame. This was continued recursively until the particle trajectory ended, either because the subsequent frame violated the above conditions or because the end of the sequence was reached. Trajectories consisting of fewer than 12 frames were discarded. In addition, for particle tracking in the nucleoplasm, the boundary of the nuclear region was determined (from averaging multiple frames), and particle trajectories that came within five pixels of the boundary were discarded. For each trajectory, the mean squared displacement MSD(t) was computed from the formula

$$\text{MSD}(t) = \frac{1}{L-n} \sum_{s=0}^{L-n-1} (\mathbf{r}(s+n) - \mathbf{r}(s))^2,$$

where $n = t/\Delta t$, L is the length of the trajectory (number of frames), and $\mathbf{r}(s)$ is the two-dimensional position of the particle in frame s. ($s = 0$

corresponds to the start of the trajectory.) To determine the diffusion constant from a trajectory, a line was fit to MSD($n\Delta t$) with n running from 1 to the largest integer less than or equal to $L/4$ (Saxton, 1997). The square of the protein displacement between adjacent frames, averaged over the protein trajectory, was computed from the formula $\langle\Delta\mathbf{r}^2\rangle_{\mathrm{traj}} = \mathrm{MSD}(\Delta t)$. For simple diffusion, the distribution of displacements or steps $\Delta\mathbf{r}$ is Gaussian, and the distribution of $\langle\Delta\mathbf{r}^2\rangle_{\mathrm{traj}}$ can be expressed in terms of the χ^2 distribution (Hoel, 1962; Qian et al., 1991). The probability that $\langle\Delta\mathbf{r}^2\rangle_{\mathrm{traj}}$ lies in the interval $(a, a + \mathrm{d}a)$ is given by

$$P_{\Delta\mathrm{r}^2}(a, L)\mathrm{d}a = \frac{(L-1)^{L-1}a^{L-2}}{(L-2)!\mu^{L-1}}\exp\left(-\frac{(L-1)a}{\mu}\right)\mathrm{d}a,$$

where μ is the mean of $\langle\Delta\mathbf{r}^2\rangle_{\mathrm{traj}}$. The predicted distribution of $\langle\Delta\mathbf{r}^2\rangle_{\mathrm{traj}}$ for the measured trajectories (assuming simple diffusion) is given by

Number of trajectories with $\langle\Delta\mathbf{r}^2\rangle_{\mathrm{traj}} \in (a, a + \mathrm{d}a)$

$$= \sum_{L} \nu(L)P_{\Delta\mathrm{r}^2}(a, L)\mathrm{d}a,$$

where $\nu(L)$ is the number of trajectories of length L.

Simulation

The simulation was designed to approximate the continuous diffusion of particles during the $\Delta t = 14$-ms exposure time of each frame. To create a sequence of N consecutive images of diffusing particles, we started with $10N$ subframes, with each subframe corresponding to a time interval $\Delta t/10$. The ith particle in the jth subframe moved a displacement $(\Delta x_j^i, \Delta y_j^i, \Delta z_j^i)$, which was determined randomly from the probability distribution:

$$\mathrm{prob}\{\Delta x_j^i \in (l - \delta l, l + \delta l)\}$$

$$= \sqrt{\frac{5}{\pi D\Delta t}}\exp\left(-\frac{l^2}{2D\Delta t/10}\right)2\delta l$$

(and similarly for Δy_j^i and Δz_j^i). The interval $2\delta l$ was equal to the size of a pixel in the plane of focus (0.15 μm). The coordinates for particle i in subframe j were thus $x^i(j) = x_0^i + \sum_{k=0}^{j}\Delta x_k^i$ (and similarly for $y^i(j)$ and $z^i(j)$). The starting points (x_0^i, y_0^i, z_0^i) were determined randomly. Simulations of $N_{\mathrm{particles}} = 50$ simultaneously diffusing particles were carried out on a region of (x, y, z) dimensions (100, 100, 66) (in units of $2\delta l$) with hard-wall boundary conditions. Image frames were then created from consecutive groups of 10 subframes, with the pixel intensity at coordinates x, y in the nth frame assigned the value

intensity(x, y, n)

$$= \mathrm{int}\left(\sum_{i=1}^{N_{\mathrm{particles}}}\sum_{j=10n}^{10n+9} 25 \exp(-z^i(j)^2/d^2)\delta_{x,x^i(j)}\delta_{y,y^i(j)}\right),$$

where int( ) denotes truncation to the nearest integer, d is a constant, and $\delta_{a, b} = 1$ if $a = b$ and 0 otherwise. The exponential factor in the above expression is included to approximate the loss of intensity as particles move away from the plane of focus (corresponding to $z = 0$). Intensities larger than 255 were set to 255 (resulting in an 8-bit grayscale). Particle trajectories were found by analyzing the sequence of images with the same software that was used for the experimental data. The parameter $D = 2.9$ μm^2/s was chosen so that the mean value of the diffusion constant measured from slopes of MSD(t) was equal to the corresponding mean diffusion constant for RPE in the cytoplasm (2.7 μm^2/s). The mean diffusion constant from the analyzed trajectories was lower than D because of biases toward slower trajectories in the analysis software (see Discussion). The

parameter $d = 0.3$ μm was similarly chosen so that the mean length of the trajectories was equal to the corresponding mean length of the experimental trajectories (17 frames). The resulting distribution of lengths of the trajectories was quite similar to the distribution of lengths for RPE in the cytoplasm (data not shown).

RESULTS

Imaging single proteins of RPE

To verify that we were detecting single proteins, we first imaged RPE adsorbed on a coverslip (Fig. 1). When images were acquired at 71 frames/s, we observed fluctuations or blinking in the fluorescence emission from single spots (Fig. 2). Similar blinking has been seen in single molecule imaging of GFP (Pierce et al., 1997; Dickson et al., 1997) and other fluorescent molecules (Trautman and Macklin, 1996; Lu and Xie, 1997) and is probably due to fluctuations in the local environment around the fluorophores. We have three lines of evidence supporting the claim that the spots in Fig. 1 are images of single proteins: 1) Histograms of peak intensities from sequences like those in Fig. 2 show a single peak (Fig. 3). This suggests that the particles have a well-defined stoichiometry. 2) The intensity from individual spots frequently jumps back and forth from maximum intensity to baseline (Fig. 2). Such transitions would be relatively rare if the spots corresponded to random protein aggregates. (Note that the fluorophores within RPE are coupled through resonance energy transfer (Glazer, 1989). It is possible that this cooperativity is partially responsible for the observed fluctuations between the maximum and zero emission.) 3) From dynamic light scattering measurements (data not shown) we found that RPE in solution consisted of particles of a single size with a Stokes radius of 5.6 nm (corresponding to a diffusion constant of 40 μm^2/s), which is comparable to the size of RPE (Ficner et al., 1992). Furthermore, on the microscope we occasionally obtained sequences of particles moving onto the coverslip from free solution. This indicates that the particles on the coverslip
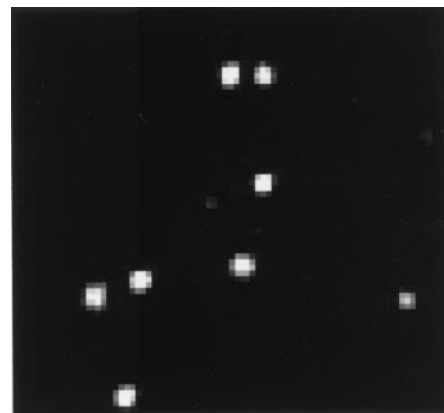

FIGURE 1   Image of RPE proteins on a coverslip: 14-ms exposure with nearest-neighbor averaging (see Materials and Methods).
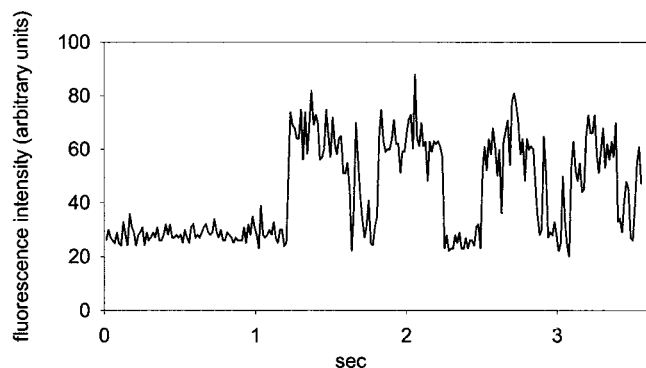
FIGURE 2 Fluctuations in fluorescence emission from a single RPE protein on a coverslip obtained from 250 consecutive 14-ms exposures.

were of the same form as the particles in solution. We therefore conclude that the spots in Fig. 1 are single proteins of RPE.

Tracking RPE in the cytoplasm

When RPE was injected into the cytoplasm of TC7 cells and images were acquired at 70 frames/s (14 ms/frame), sequences were obtained showing the motion of distinct proteins. Using our own image analysis software, particle positions were determined from intensity maxima, and trajectories were identified (see Materials and Methods). The analysis of these trajectories was complicated by the fact that we only measured the lateral (x-y) displacement of the proteins, corresponding to the projection of the protein trajectories onto the plane of focus. There were three factors that potentially limited the amount of time that RPE could be tracked with this approach: photobleaching, fluorescence fluctuations, and motion in the z (vertical) direction. From sequences of images of cells containing a large number of RPE proteins, we measured the total fluorescence intensity as a function of time under continuous illumination. The
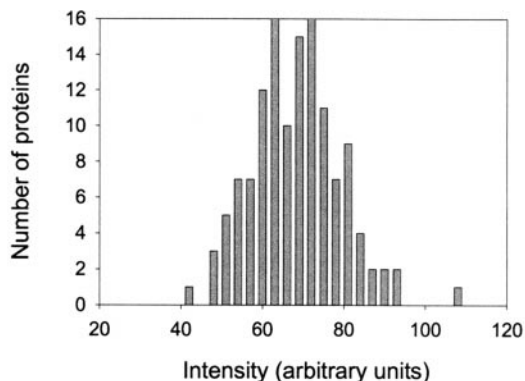

FIGURE 3 Histogram of peak intensity for RPE proteins adsorbed on a coverslip.

resulting curves are well described by an exponential decay, with a time constant of 3 s (data not shown). Thus proteins under continuous illumination from the excitation source had mean lifetimes of ~ 3 s before they were photobleached. Another factor that could limit trajectory length was the fluctuations in RPE fluorescence emission described above. When the fluorescence from a single RPE protein dropped to a value comparable to the background fluorescence as a result of these fluctuations, the protein could no longer be detected. To get a bound on the typical time for this to happen, we used our particle-tracking program to identify (static) trajectories for RPE imaged on coverslips. The mean number of consecutive frames for which a single RPE could be detected above background was 40 ($n = 87$), which corresponds to 560 ms. The corresponding value for RPE in cells would be lower, however, because of the higher background fluorescence. The final factor that could limit trajectory length was the disappearance of proteins that moved too far out of the plane of focus. We were able to detect particles within a depth d above and below the plane of focus. This distance depends on the depth of field of the objective lens, which determines how rapidly the peak intensity in the image drops as the protein moves away from the plane of focus, and on the background fluorescence, which sets the minimum intensity for which we are able to detect proteins. If the proteins were characterized by a diffusion constant D, then the typical time for which they could be tracked before they moved too far from the plane of focus was $\sim d^2/D$. As a rough estimate, if we take $d \approx 1$ μm and $D \approx 3$ μm^2/s, we get a time of ~ 0.3 s or ~ 20 frames. Note that for systems consisting of particles with different diffusion constants, there will be a bias toward detecting longer trajectories for the slower particles. This is a result of the tendency for the faster particles to move away from the plane of focus more rapidly, as well as the fact that the image of the faster particles will have a lower intensity per pixel because the particles transit more pixels in the course of the 14-ms exposure for each frame.

At least for the fraction of RPE proteins that were moving sufficiently slowly for their trajectories to be detectable, we were able to obtain trajectories consisting of 12–50 frames (14 ms/frame), with an average of 17 frames. (The lower bound of 12 was chosen to ensure that each trajectory had enough points to determine the mean squared displacement for a reasonable number of time points.) This range suggests that both blinking and motion in z were responsible for limiting the number of frames for which proteins could be tracked and that photobleaching was not a significant limitation.

An analysis of the distributions of the mean velocities and of the velocity-velocity autocorrelation functions for the acquired trajectories did not show any evidence of directed or correlated motion (data not shown), which suggests that the displacement in each frame was not correlated with the

displacement in the previous frame for each particle. To extract information about the mobilities of the proteins, we computed the mean squared displacement MSD(t) for each trajectory (see Materials and Methods). For long trajectories of particles undergoing simple diffusion with diffusion constant D, MSD(t) = $4Dt$. (The factor of 4 applies for two-dimensional trajectories, including projections of three-dimensional simple diffusion onto a plane.) For short trajectories, however, MSD(t) has relatively large statistical fluctuations. In this case, linear fits to MSD(t) will give a distribution of diffusion constants (Qian et al., 1991; Saxton, 1997). We determined the distribution of D from the slopes of linear fits to MSD(t) for 978 trajectories of RPE proteins moving in the cytoplasm (Fig. 4 a). The distribution is quite broad, with a mean value of 2.7 μm^2/s. As has been emphasized by Qian et al. (1991) and Saxton (1997), to draw conclusions about particle motion from single particle tracking data, it is important to compare the results with distributions from other experimental systems or from theoretical models. We therefore also tracked single proteins of RPE in free solution and carried out Monte Carlo simulations of simple diffusion.

The Monte Carlo simulation was used to generate sequences of images of particles diffusing in a three-dimensional volume (see Materials and Methods). The intensity of each particle was taken to be maximal at $z = 0$ (corresponding to the plane of focus) and fell off with deviations from $z = 0$ with a Gaussian profile. As for the case of the experimental data, particles sufficiently far from the plane of focus had intensities below the threshold of detection. The sequences of images were analyzed with the same particle tracking software that was used for the experimentally acquired sequences. The distribution of lengths of the resulting trajectories was comparable to the distribution obtained for RPE in the cytoplasm (data not shown). However, the resulting distribution of diffusion constants (with a mean value of $D = 2.7$ μm^2/s) was clearly narrower than the distribution for intracellular RPE (Fig. 4, b and d).
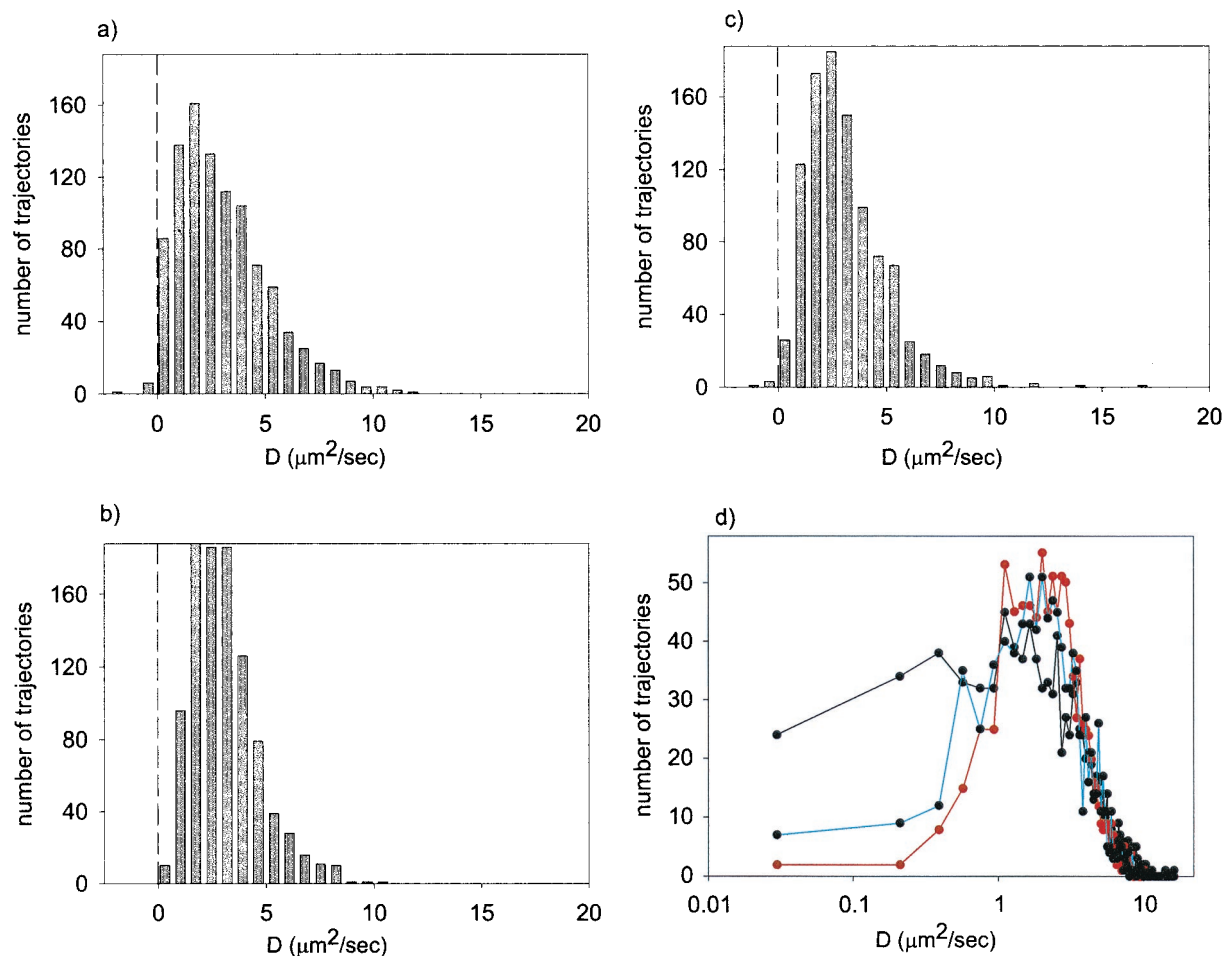

FIGURE 4   Histograms of 978 diffusion constants determined from linear fits to MSD(t) for each trajectory for RPE in the cytoplasm (a), simulation of simple diffusion (b), and RPE in glycerol (c). All three distributions have mean values of 2.7 μm^2/s. (d) Semilog plot of the three distributions (positive values only). RPE in the cytoplasm (*black*), simulation (*red*), RPE in glycerol (*blue*).

To track RPE in free solution, we decreased the diffusion constant by adding glycerol to a dilute solution of the protein. We then acquired and analyzed image sequences with the same procedure that was used for intracellular RPE. In a solution of 50% glycerol the average diffusion constant for RPE (from a linear fit to MSD(t)) was 2.7 μm^2/s, which is the value we obtained in the cytoplasm. However, as was seen with the simulation, the corresponding distribution of D was narrower than the distribution for RPE in the cytoplasm (Fig. 4, c and d). By applying the Kolmogorov-Smirnov test (Press et al., 1993), we find the probability that the data for RPE in the cytoplasm (Fig. 4 a) and in glycerol (Fig. 4 c) are described by different distributions is >99.9%.

The particle trajectories may be thought of as two-dimensional random walks in which each particle takes a step corresponding to a displacement $\Delta \mathbf{r}$ in each frame. For each particle, the square of the displacements averaged over a particle's trajectory is related to the diffusion constant by $\langle \Delta \mathbf{r}^2 \rangle_{\text{traj}} = 4D\Delta t$, where Δt is the time between steps. Again this relation strictly holds only in the limit of infinite trajectories; for finite trajectories there will be statistical fluctuations. Although the above relation holds if the particle positions are determined from instantaneous snapshots, there is a correction for the case described here. This is because each image that we acquired had a finite (14-ms) exposure time and thus contained information about particle positions over the entire $\Delta t = 14$ ms and not about the positions at a single instant. If we were to use the mean position of a particle in each frame, then the correct formula would be $\langle \Delta \mathbf{r}^2 \rangle_{\text{traj}} = 4(2D/3)\Delta t$ (see the Appendix). However, we determined each particle's position by using the mean of the intensity maxima in each frame. (The background fluorescence and intensifier noise were too high to determine the positions from the mean of all pixels occupied by a protein during the 14-ms exposure.) As a result, the relation will take the form $\langle \Delta \mathbf{r}^2 \rangle_{\text{traj}} = 4D'\Delta t$, with D' between $2D/3$ and D. The quantity $\langle \Delta \mathbf{r}^2 \rangle_{\text{traj}}$ (or, equivalently, D') is useful because we can compute its theoretical distribution for the case of simple diffusion (see Materials and Methods). For the simulation described above, the distribution of D' is fit well by the theoretical distribution (Fig. 5 b). Note that the mean value of $D' = 2.3$ μm^2/s is lower than $D = 2.7$ μm^2/s, as expected. For cytoplasmic RPE, on the other hand, the distribution of D' is much broader than the theoretical distribution (Fig. 5 a). Note in addition that the mean value of $D' = 3.5$ μm^2/s is larger than the mean $D = 2.7$ μm^2/s obtained from linear fits to MSD(t). For RPE in glycerol, the distribution of D' is reasonably well fit by the theoretical distribution (Fig. 5 c), at least relative to the case of cytoplasmic RPE. Again, the mean value of $D' = 4.1$ μm^2/s is larger than the mean $D = 2.7$ μm^2/s obtained from linear fits to MSD(t); we will return to this point below in the Discussion.
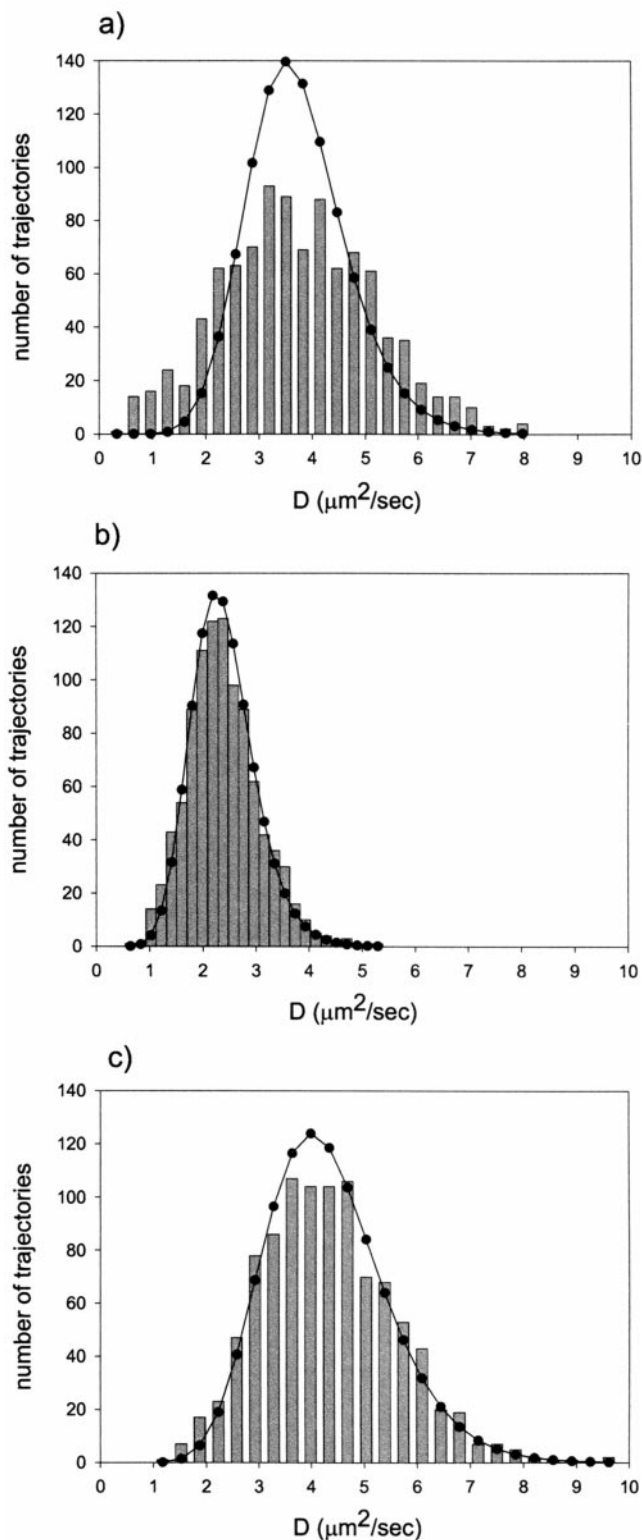

FIGURE 5 Distribution of diffusion constants determined from $D' \equiv \langle \Delta \mathbf{r}^2 \rangle_{\text{traj}}/4\Delta t$ (*vertical bars*) and the predicted distributions assuming simple diffusion (*black dots*). (*a*) RPE in the cytoplasm, mean = 3.5 μm^2/s. (*b*) Simulation of simple diffusion, mean = 2.3 μm^2/s. (*c*) RPE in glycerol, mean = 4.1 μm^2/s.

Tracking RPE in the nucleoplasm

We were also able to track single proteins after microinjecting RPE into the nucleus. Injection into such a small volume may create severe disruptions of the nuclear environment, which could significantly affect the mobility of RPE. We therefore also took a second approach in which we chemically conjugated a nuclear localization sequence (NLS) to RPE to load the nucleus in a less disruptive manner. After microinjection into the cytoplasm, RPE-NLS accumulated in the nucleus (Fig. 6). Sequences were acquired and analyzed in the same manner as for cytoplasmic RPE. The average trajectory length was 16 frames for both nuclear RPE and RPE-NLS. We again found broad distributions for diffusion constants obtained from linear fits to MSD(t) for both RPE (Fig. 7 *a*) and RPE-NLS (Fig. 7 *b*), with mean values of $D = 1.1$ $\mu m^2/s$ and $D = 1.7$ $\mu m^2/s$, respectively. The distributions of D' (obtained from $\langle \Delta \mathbf{r}^2 \rangle_{\text{traj}}$) for nuclear RPE (Fig. 8 *a*) and RPE-NLS (Fig. 8 *b*) were also much broader than the predicted distributions.

DISCUSSION

By taking advantage of the bright fluorescence of RPE, we have been able to track single proteins moving in the cytoplasm and nucleoplasm of TC7 cells for an average of 17 (cytoplasm) or 16 (nucleoplasm) frames at 14 ms/frame. The lengths of the acquired trajectories were limited by fluctuations in the fluorescence emission from single proteins of RPE and from the motion of the proteins out of the plane of focus. For short trajectories, averaged quantities have large statistical fluctuations. It is therefore important to present distributions of diffusion constants rather than simply mean values (Saxton, 1997; Qian et al., 1991). We have
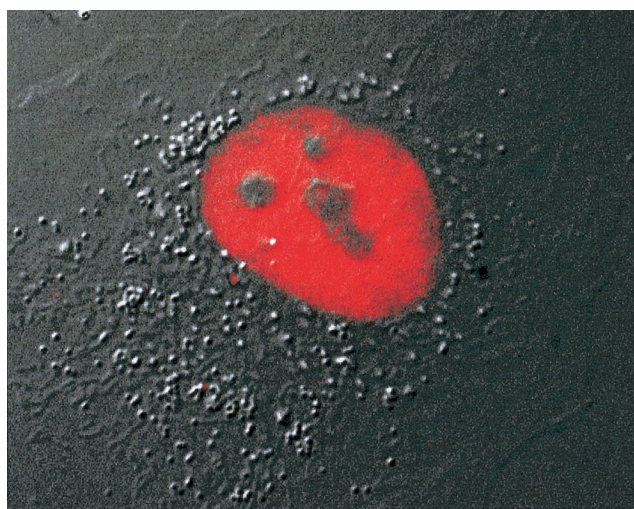
used two quantities to characterize protein trajectories: the average step squared $\langle \Delta \mathbf{r}^2 \rangle_{\text{traj}}$ and the slope of a linear fit to the mean squared displacement MSD(t). The former quantity is equal to MSD(Δt), where Δt is the inverse frame rate (14 ms). We use the term "simple diffusion" to describe the Brownian motion of particles with a constant mobility in the absence of any potentials or constraints. For simple diffusion in three dimensions, the projection of particle trajectories onto a plane (the plane of focus, in our case) reduces the system to simple diffusion in two dimensions. The resulting two-dimensional trajectories will satisfy MSD(t) = $4Dt$ (and $\langle \Delta \mathbf{r}^2 \rangle_{\text{traj}} \equiv \text{MSD}(\Delta t) = 4D\Delta t$). There are a number of ways in which systems can deviate from simple diffusion. These include systems with directed motion, confined motion, and diffusion with space- or time-dependent mobilities. In all of these cases, MSD(t) will not be linear in t, at least over some time scales (see Saxton and Jacobson, 1997, and references therein).

For RPE in the cytoplasm, we obtained distributions for diffusion constants (derived from $\langle \Delta \mathbf{r}^2 \rangle_{\text{traj}}$ and slopes of MSD(t)) that were broader than the distributions obtained for RPE in a glycerol solution with the same mean diffusion constant and from simulated and theoretical distributions for simple diffusion. The distributions of diffusion constants for RPE and RPE-NLS in the nucleoplasm were similarly broader than those expected for simple diffusion. The broad distributions indicate that over the time scales in our experiments ($\sim$10–100 ms), the motion of RPE does not correspond to simple diffusion with a unique diffusion constant in either the cytoplasm or the nucleoplasm. With the present data, however, we cannot determine if the system is best characterized by a few diffusion constants, a continuous distribution, or more complex behavior, such as confined or anomalous diffusion (see, e.g., Saxton and Jacobson, 1997).

The resolution of particle position in our measurements was limited by noise from the image intensifier and fluctuations in background fluorescence. In particular, when we acquired trajectories of static RPE (on coverslips), the trajectories show fluctuations in the range of one to two pixels around fixed points (data not shown). (One pixel corresponds to a distance of 0.15 μm in the plane of focus.) A stationary subpopulation of RPE within cells would appear as a peak near zero in the histogram for D. Thus, the large number of trajectories with D near zero for cytoplasmic RPE relative to simulation and RPE in glycerol (Fig. 4 *d*) could in part reflect the presence of a stationary subpopulation. However, stationary RPE cannot account for the entire difference between distributions. For RPE immobilized on coverslips, the distribution is peaked at values much closer to the origin than what is observed for cytoplasmic RPE. As a result, if immobile RPE within cells played a significant role in skewing the distribution of D to low values, then there would be a second peak in the lowest bin in Fig. 4 *d*.

FIGURE 6 Combined fluorescence (*red*) and differential interference contrast images of a TC7 cell showing accumulation of RPE-NLS in the nucleus after injection in the cytoplasm.

FIGURE 7 Histograms of diffusion constants from linear fits to the MSD(t) proteins in the nucleoplasm. (*a*) RPE, mean = 1.1 μm^2/s, 287 trajectories. (*b*) RPE-NLS, mean = 1.7 μm^2/s, 145 trajectories.
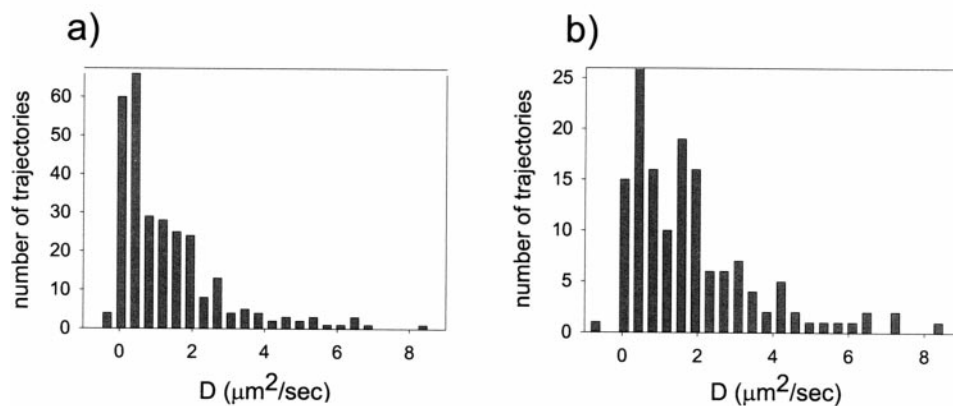
The diffusion constant of RPE has been measured by FRAP to be 4.6 ± 1.1 μm^2/s and 4.4 ± 1.3 μm^2/s in the cytoplasm and nucleoplasm, respectively (Schulz and Peters, 1987). These values are higher than the values we obtained from taking means of the single-particle data (D = 2.7 μm^2/s for cytoplasmic RPE, 1.1 μm^2/s for nucleoplasmic RPE, 1.7 μm^2/s for nucleoplasmic RPE-NLS). The experiments of Schulz and Peters (1987) were performed on HTC cells instead of on TC7 cells, which could account for part of the discrepancy. However, the most likely explanation is that our means are lower because of the bias toward slow trajectories in our analysis. It is difficult to identify trajectories for proteins moving too quickly. Even when the protein remains within the field of view, if it has moved too far in two successive frames, then it is no longer clear whether it is the same protein. Note that this bias toward slow trajectories indicates that the actual distributions are even broader than those measured here.

As discussed in the Appendix, for trajectories acquired from images with a finite exposure time, the average value of $D' = \langle \Delta \mathbf{r}^2 \rangle_{\text{traj}}/(4\Delta t)$ is lower than the average value of the diffusion constant D obtained from linear fits to MSD(t). This is evident for the case of our simulation. For both RPE in glycerol and intracellular RPE, however, D' is greater than D. This is most likely due to the fluctuations in background fluorescence and intensifier noise, which will result in fluctuations about the correct particle positions. These fluctuations average out over long time scales. Hence, a linear fit to MSD(t) will be less sensitive to these fluctuations than will $\langle \Delta \mathbf{r}^2 \rangle_{\text{traj}}$, which measures deviations on the shortest time scale Δt.

For diffusion in the cytoplasm, the most likely explanation for the variation in protein mobility is that it stems from interactions of RPE with intracellular constituents such as the cytoskeleton, membranes, or high concentrations of other macromolecules, mobile or immobile, within the cell
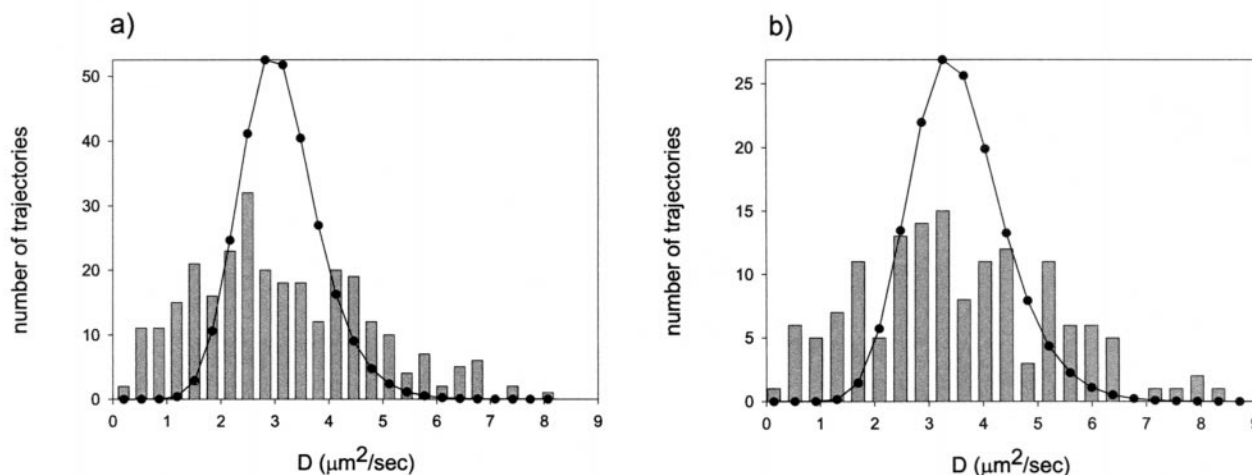

FIGURE 8 Distribution of diffusion constants determined from $D' \equiv \langle \Delta \mathbf{r}^2 \rangle_{\text{traj}}/4\Delta t$ (*vertical bars*) and the predicted distributions, assuming simple diffusion (*black dots*). (*a*) RPE in the nucleoplasm, mean = 2.6 μm^2/s. (*b*) RPE-NLS in the nucleoplasm, mean = 3.2 μm^2/s.

(see, e.g., Luby-Phelps et al., 1986; Zimmerman and Minton, 1993; Luby-Phelps, 2000). These assemblies could act as obstacles that impede the motion of soluble proteins or, alternatively, provide a dense collection of sites to which RPE transiently binds. This would account for the fact that intracellular diffusion constants are lower than the corresponding free solution values (Jacobson and Wojcieszyn, 1984; Luby-Phelps et al., 1986, 1987; Lang et al., 1986; Arrio-Dupont et al., 1996, 2000; Seksek et al., 1997; Lukacs et al., 2000).

The fact that we observe what appears to be a range of mobilities for RPE suggests that different RPE proteins experience different average environments over the length and time scales probed by our experiments. This could be due to a heterogeneous distribution of the material responsible for slowing RPE. Alternatively, the probability of RPE interacting strongly with intracellular components could be sufficiently low that the fluctuations in mobility due to these interactions are large. The situation is similar to the case of two-dimensional diffusion in the plasma membrane, where single particle tracking has also revealed a broad distribution of diffusion coefficients (Kusumi et al., 1993; Lee et al., 1993; Sako and Kusumi, 1994; Saxton and Jacobson, 1997). In this case it has been suggested that the variation in mobilities is due to interactions with the membrane skeleton, the extracellular matrix, or membrane microdomains (reviewed in Saxton and Jacobson, 1997). Models of two-dimensional diffusion in the presence of obstacles and binding sites and the resulting distributions of diffusion coefficients have been explored by Saxton (1997). Models of anomalous diffusion in obstructed geometries in three dimensions have been applied to diffusion in organelles by Olveczky and Verkman (1998).

Much less is known about the structure of the nucleoplasm than about the structure of the cytoplasm (Pederson, 1998). Again, FRAP experiments demonstrate that diffusion is slower in the nucleus than in free solution (Lang et al., 1986; Schulz and Peters, 1987; Seksek et al., 1997; Politz et al., 1998). Our single particle tracking data indicate that nuclear RPE and RPE-NLS are not characterized by simple diffusion, based on a comparison with the predicted distribution for $\langle \Delta \mathbf{r}^2 \rangle_{\text{traj}}$. Interestingly, we find that the distributions of diffusion constants for RPE and RPE-NLS are comparable. This suggests that interactions between the positively charged NLS with DNA, transport factors, or other nuclear proteins do not significantly affect the mobility within the nucleus. The mechanism for accumulation of NLS bearing proteins in the nucleus is not understood. One class of models is based on the idea of nuclear retention (Paine, 1993, and references therein), in which the NLS binds to constituents of the nucleus in such a way that diffusion of protein-NLS out of the nucleus is prevented. Although our results do not rule out these models, they indicate that any potential interactions leading to nuclear retention do not restrict the mobility of the protein-NLS.

The experiments described here provide the first example of intracellular single protein tracking. With improvements in the experimental system, this technique could provide a wealth of information on protein mobility within the cell. Increased sensitivity and frame acquisition rate, as well as particle tracking in three dimensions, will result in better statistical sampling and allow comparisons with specific models of diffusive transport. In addition, by microinjecting RPE that has been conjugated to other proteins, or possibly conjugating RPE to a protein of interest directly within the cell (Farinas and Verkman, 1999), it may be possible to track endogenous proteins. The single particle tracking experiments described here are a first step toward probing intracellular processes at the single protein level.

APPENDIX

In this appendix we consider the analysis of a diffusing particle in which the data consist of consecutive images with finite exposure times Δt. The particle position in the jth image, $\mathbf{r}(t)$ with $t = j\Delta t$, is taken to be the mean of the intensity-weighted position (center of mass) in the image. Let $\mathbf{R}(t)$ denote the trajectory of a random particle, which satisfies $\langle (\mathbf{R}(t) - \mathbf{R}(t')^2) \rangle = 4D|t - t'|$, ($\langle \ \rangle$ denotes averaging over the trajectory). To approximate $\mathbf{r}(t)$ we divide the interval Δt into n subintervals of width ε ($\Delta t = n\varepsilon$) and define

$$\mathbf{r}(t) \equiv \frac{1}{n} \sum_{m=0}^{n-1} \mathbf{R}(t + m\varepsilon).$$

We then have for $t' \geq t + n\varepsilon$

$$\langle (\mathbf{r}(t) - \mathbf{r}(t'))^2 \rangle$$

$$= \frac{1}{n^2} \sum_{m_1, m_2=0}^{n-1} \langle (\mathbf{R}(t + m_1\varepsilon) - \mathbf{R}(t' + m_1\varepsilon))(\mathbf{R}(t + m_2\varepsilon) $$
$$- \mathbf{R}(t' + m_2\varepsilon)) \rangle$$

$$= \frac{1}{2n^2} \sum_{m_1, m_2} 2\langle (\mathbf{R}(t + m_1\varepsilon) - \mathbf{R}(t' + m_2\varepsilon))^2 \rangle$$

$$- \langle (\mathbf{R}(t + m_1\varepsilon) - \mathbf{R}(t + m_2\varepsilon))^2 \rangle$$

$$- \langle (\mathbf{R}(t' + m_1\varepsilon) - \mathbf{R}(t' + m_2\varepsilon))^2 \rangle$$

$$= \frac{4D}{n^2} \sum_{m_1, m_2} (t' - t + m_2\varepsilon - m_1\varepsilon - |m_1 - m_2|\varepsilon)$$

$$= 4D\left(t' - t - \frac{n^2 - 1}{3n}\varepsilon\right).$$

For the mean square displacement we take $t' - t = k\Delta t$, set $\varepsilon = \Delta t/n$, and take $n \to \infty$ to give

$$\text{MSD}(k\Delta t) = 4D\Delta t(k - \tfrac{1}{3}).$$

Thus, the slopes of linear fits to MSD(t) will give the correct diffusion constant, although one should not include the origin in a linear fit to the data. For the mean displacement between adjacent images (the mean step squared), on the other hand, we have

$$\langle (\Delta \mathbf{r})^2 \rangle_{\text{traj}} = \text{MSD}(\Delta t) = 4(\tfrac{2}{3}D)\Delta t \equiv 4D'\Delta t.$$

Thus, the diffusion constant satisfies $D = 3D'/2$. If the particle location is determined from a subset of the points occupied by the particle during the frame exposure time (e.g., the center of mass of pixels of maximum intensity), then D will be between D' and $3D'/2$.

REFERENCES

Arrio-Dupont, M., S. Cribier, G. Foucault, P. F. Devaux, and A. d'Albis. 1996. Diffusion of fluorescently labeled macromolecules in cultured muscle cells. *Biophys. J.* 70:2327–2332.

Arrio-Dupont, M., G. Foucault, M. Vacher, P. F. Devaux, and S. Cribier. 2000. Translational diffusion of globular proteins in the cytoplasm of cultured muscle cells. *Biophys. J.* 78:901–907.

Cherry, R. J., K. M. Wilson, K. Triantafilou, P. O'Toole, I. E. Morrison, P. R. Smith, and N. Fernandez. 1998. Detection of dimers of dimers of human leukocyte antigen (HLA)-DR on the surface of living cells by single-particle fluorescence imaging. *J. Cell Biol.* 140:71–79.

Dickson, R. M., A. B. Cubitt, R. Y. Tsien, and W. E. Moerner. 1997. On/off blinking and switching behaviour of single molecules of green fluorescent protein. *Nature.* 388:355–358.

Farinas, J., and A. S. Verkman. 1999. Receptor-mediated targeting of fluorescent probes in living cells. *J. Biol. Chem.* 274:7603–7606.

Ficner, R., K. Lobeck, G. Schmidt, and R. Huber. 1992. Isolation, crystallization, crystal structure analysis and refinement of B-phycoerythrin from the red alga *Porphyridium sordidum* at 2.2 Å resolution. *J. Mol. Biol.* 228:935–950.

Freshney, R. I. 1994. Culture of Animal Cells: A Manual of Basic Technique. Wiley-Liss, New York.

Fushimi, K., and A. S. Verkman. 1991. Low viscosity in the aqueous domain of cell cytoplasm measured by picosecond polarization microfluorimetry. *J. Cell Biol.* 112:719–725.

Glazer, A. N. 1982. Phycobilisomes: structure and dynamics. *Annu. Rev. Microbiol.* 36:173–198.

Glazer, A. N. 1988. Phycobiliproteins. *Methods Enzymol.* 167:291–303.

Glazer, A. N. 1989. Light guides. Directional energy transfer in a photosynthetic antenna. *J. Biol. Chem.* 264:1–4.

Gordon, G. W., B. Chazotte, X. F. Wang, and B. Herman. 1995. Analysis of simulated and experimental fluorescence recovery after photobleaching. Data for two diffusing components. *Biophys. J.* 68:766–778.

Hoel, P. G. 1962. Introduction to Mathematical Statistics. John Wiley and Sons, New York.

Jacobson, K., and J. Wojcieszyn. 1984:The translational mobility of substances within the cytoplasmic matrix. *Proc. Natl. Acad. Sci. USA.* 81:6747–6751.

Kegel, W. K. and A. van Blaaderen. 2000. Direct observation of dynamical heterogeneities in colloidal hard- sphere suspensions. *Science.* 287: 290–293.

Kusumi, A., Y. Sako, and M. Yamamoto. 1993. Confined lateral diffusion of membrane receptors as studied by single particle tracking (nanovid microscopy). Effects of calcium-induced differentiation in cultured epithelial cells. *Biophys. J.* 65:2021–2040.

Lang, I., M. Scholz, and R. Peters. 1986. Molecular mobility and nucleocytoplasmic flux in hepatoma cells. *J. Cell Biol.* 102:1183–1190.

Lee, G. M., F. Zhang, A. Ishihara, C. L. McNeil, and K. A. Jacobson. 1993. Unconfined lateral diffusion and an estimate of pericellular matrix viscosity revealed by measuring the mobility of gold-tagged lipids. *J. Cell Biol.* 120:25–35.

Lu, H. P. and X. S. Xie. 1997. Single-molecule spectral fluctuations at room temperature. *Nature.* 385:143–146.

Luby-Phelps, K. 1994. Physical properties of cytoplasm. *Curr. Opin. Cell Biol.* 6:3–9.

Luby-Phelps, K. 2000. Cytoarchitecture and physical properties of cytoplasm: volume, viscosity, diffusion, intracellular surface area. *Int. Rev. Cytol.* 192:189–221.

Luby-Phelps, K., P. E. Castle, D. L. Taylor, and F. Lanni. 1987. Hindered diffusion of inert tracer particles in the cytoplasm of mouse 3T3 cells. *Proc. Natl. Acad. Sci. USA.* 84:4910–4913.

Luby-Phelps, K., S. Mujumdar, R. B. Mujumdar, L. A. Ernst, W. Galbraith, and A. S. Waggoner. 1993. A novel fluorescence ratiometric method confirms the low solvent viscosity of the cytoplasm. *Biophys. J.* 65: 236–242.

Luby-Phelps, K., D. L. Taylor, and F. Lanni. 1986. Probing the structure of cytoplasm. *J. Cell Biol.* 102:2015–2022.

Lukacs, G. L., P. Haggie, O. Seksek, D. Lechardeur, N. Freedman, and A. S. Verkman. 2000. Size-dependent DNA mobility in cytoplasm and nucleus. *J. Biol. Chem.* 275:1625–1629.

Olveczky, B. P. and A. S. Verkman. 1998. Monte Carlo analysis of obstructed diffusion in three dimensions: application to molecular diffusion in organelles. *Biophys. J.* 74:2722–2730.

Paine, P. 1993. Nuclear protein accumulation by facilitated transport and intranuclear binding. *Trends Cell Biol.* 3:325–329.

Pederson, T. 1998. Thinking about a nuclear matrix. *J. Mol. Biol.* 277: 147–159.

Periasamy, N., and A. S. Verkman. 1998. Analysis of fluorophore diffusion by continuous distributions of diffusion coefficients: application to photobleaching measurements of multicomponent and anomalous diffusion. *Biophys. J.* 75:557–567.

Pierce, D. W., N. Hom-Booher, and R. D. Vale. 1997. Imaging individual green fluorescent proteins. *Nature.* 388:338.

Politz, J. C., E. S. Browne, D. E. Wolf, and T. Pederson. 1998. Intranuclear diffusion and hybridization state of oligonucleotides measured by fluorescence correlation spectroscopy in living cells. *Proc. Natl. Acad. Sci. USA.* 95:6043–6048.

Press, W. H., S. A. Teukolsky, W. T. Vetterling, and B. P. Flannery. 1993. Numerical Recipes in C: The Art of Scientific Computing. Cambridge University Press, New York.

Qian, H., M. P. Sheetz, and E. L. Elson. 1991. Single particle tracking. Analysis of diffusion and flow in two-dimensional systems. *Biophys. J.* 60:910–921.

Sako, Y., and A. Kusumi. 1994. Compartmentalized structure of the plasma membrane for receptor movements as revealed by a nanometer-level motion analysis. *J. Cell Biol.* 125:1251–1264.

Saxton, M. J. 1997. Single-particle tracking: the distribution of diffusion coefficients. *Biophys. J.* 72:1744–1753.

Schulz, B., and R. Peters. 1987. Nucleocytoplasmic protein traffic in single mammalian cells studied by fluorescence microphotolysis. *Biochim. Biophys. Acta.* 930:419–431.

Seksek, O., J. Biwersi, and A. S. Verkman. 1997. Translational diffusion of macromolecule-sized solutes in cytoplasm and nucleus. *J. Cell Biol.* 138:131–142.

Trautman, J. K., and J. J. Macklin. 1996. Time-resolved spectroscopy of single molecules using near-field and far-field optics. *J. Chem. Phys.* 205:221–229.

Weeks, E. R., J. C. Crocker, A. C. Levitt, A. Schofield, and D. A. Weitz. 2000. Three-dimensional direct imaging of structural relaxation near the colloidal glass transition. *Science.* 287:627–631.

Wilson, K. M., I. E. Morrison, P. R. Smith, N. Fernandez, and R. J. Cherry. 1996. Single particle tracking of cell-surface HLA-DR molecules using R-phycoerythrin labeled monoclonal antibodies and fluorescence digital imaging. *J. Cell Sci.* 109:2101–2109.

Wolf, D. E. 1989. Designing, building, and using a fluorescence recovery after photobleaching instrument. *Methods Cell Biol.* 30:271–306.

Zimmerman, S. B. and A. P. Minton. 1993. Macromolecular crowding: biochemical, biophysical, and physiological consequences. *Annu. Rev. Biophys. Biomol. Struct.* 22:27–65.